

Spontaneous charge polarization in single-electron tunneling through coupled nanowires

A. A. Tager* and J. M. Xu

Electrical & Computer Engineering Department, University of Toronto, 10 King's College Road, Toronto, Ontario, Canada M5S 1A4

M. Moskovits

Department of Chemistry, University of Toronto, 80 St. George Street, Toronto, Ontario, Canada M5S 1A4

(Received 3 September 1996)

Recent observations of periodic anomalies in conductance of two-dimensional arrays of densely packed metal or semiconductor nanowires give some indication on the importance of collective charge excitations in such systems. These structures can be viewed as parallel arrays of double-tunnel-junction systems with nanowires in the middle which are electrostatically coupled to each other. To assess possible effects of the interwire coupling on the electron transport in such arrays, we investigate the electrical behavior of a simpler system of two coupled double-junction systems under the condition of Coulomb-controlled tunneling. Using Monte Carlo simulations of the electron transport through the system and the master equation analysis, we find that a system of two coupled nanowires exhibits a spontaneous polarization of charge where the accumulation of excessive electrons on one wire is accompanied by the hole accumulation on the neighboring wire. This yields considerable net charge polarization in the transverse direction, which stochastically oscillates in time but depends periodically on the applied voltage, with both the average polarization and the polarization noise decreasing with increasing temperature. The effect gives rise to a number of changes to the well-known Coulomb-Blockade features of a double-junction system, and may lead to the appearance of periodic polarization structures or polarization waves in nanowire arrays which might be detected externally.

[S0163-1829(97)09007-3]

I. INTRODUCTION

Recently, a method of making nanostructures by electrochemical deposition of materials of interest into an array of self-organized pores in anodized aluminum oxide films has been developed.¹⁻³ These nanowire templates, when sandwiched in-between metal/oxide layers, form two-dimensional arrays of double-junction systems (Fig. 1). At room temperature these arrays exhibit a great variety of promising device behaviors and interesting phenomena, including both periodic and anomalous conductance oscillations, as well as staircase I - V behavior resembling the characteristics of single-electron tunneling (SET).⁴ The task of understanding the behavior of these nanowire devices turns out to be as challenging as making them, or even more so. It is complicated both by the fact that most of the origins of the observed phenomena are yet to be identified, and by the fact that this nonlithographic nanofabrication technique is at its infancy and inevitably suffers from unintentional (often not yet known or identifiable) variations as well as the lack of precise knowledge of some key structure parameters. Resembling the situation of the early days of the now celebrated semiconductor technology itself, this calls for step-by-step methodological investigations of a range of interesting physical effects at both the experimental and theoretical fronts. Although a complete theory is out of our reach, and any explanation of the experimental results must remain speculative at the present time, progress may still be made by building up a basic understanding of the key intrinsic effects and critical features of this new class of nanodevices.

One of the important features of these nanoarrays is clearly the *electrostatic coupling* between nanowires, which

is common to all the nanowire devices fabricated this way. This coupling may affect different aspects of the nanowire device behavior, with probably the most exciting prospect of self-organized 2D charge structures which might appear in an array due to the Coulomb interactions between wires. Such a self-organized electrical polarization of the wires, if it exists, should affect electronic transport through the array, and possibly might lead to steps for I - V characteristics such as those observed experimentally. Note that the system under consideration differs in many important aspects from the previously investigated in-plane 2D arrays of tunneling junctions connected in series, where the cotunneling in the Coulomb-blockade regime leads to excitonlike behavior.⁵

In the present work, we will examine theoretically the effect of interwire coupling in one particular situation pertinent to nanostructures—under conditions of Coulomb-controlled tunneling (or SET). We will further narrow our focus to a model system of two electrostatically coupled

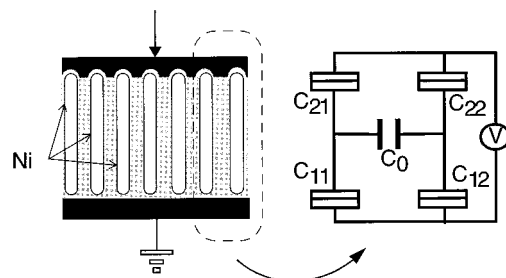


FIG. 1. Two-wire double-junction system. Arrows show the prevailing directions of tunneling for $V > 0$.

nanowires connected in parallel on the top and bottom via nanoscale tunnel junctions. This system, though greatly simplified, is, however, a basic building block of the overall device (Fig. 1), and its behavior can give some important insights into what may happen in the nanowire arrays. Results of the present study show that this seemingly simple system manifests quite interesting behavior different in many ways from that of an ordinary double-junction system, while providing an example of spontaneous creation of the transverse charge polarization in coupled nanowire systems.^{6,7} Electron transport in a somewhat similar system of two coupled multijunction chains with mutually isolated outer terminals was considered previously,⁸ but mainly in the Coulomb blockade regime when the cotunneling effects play the most important role, and in the case of weak coupling where there is no self-polarization effect.

II. MODEL SYSTEM OF COUPLED WIRES

We will investigate the electric behavior of two metallic nanowires imbedded in an oxide and contacted from top and bottom by common electrodes. We will consider the oxide as an ideal dielectric, and any exchange of electrons between contacts and wires goes through the tunneling junctions. Further, we assume that there is no electron exchange between wires since they are well separated (>30 nm typically). However, the wires are coupled electrostatically, and we are going to investigate possible consequences of this coupling in the SET regime. The junction under a positive potential will be called *the drain junction*, and the other one *the source junction*. These notations reflect the *prevailing* direction of tunneling, although for finite temperatures electrons tunnel in both directions.

Current through the system is governed by the tunneling rates $\tilde{\Gamma}_{ij}$ and $\tilde{\Gamma}_{ji}$, where the first index specifies the junction (“1” for the source and “2” for the drain), and the second one the wire, and the arrows show the direction of tunneling. According to the so-called *global rule* of the orthodox theory,^{9,10} tunneling rates depend on the differences in the total electrostatic energy of the system before and after a tunneling event \mathbf{E}_{ij} , which depends on the applied voltage V and wire charges $Q_{1,2} = -eN_{1,2}$, with the elementary charge e and number of the excess electrons on the j th wire N_j . At finite temperature T these tunneling rates in the case of low-impedance environment are given by^{9,10}

$$\Gamma_{ij} = \frac{1}{e^2 R_{ij}} \frac{E_{ij}}{1 - \exp(-E_{ij}/kT)}, \quad (1)$$

where R_{ij} are the tunneling resistances.

Straightforward calculations using equivalent model of Fig. 1 with junction capacitances C_{ij} and interwire coupling capacitance C_0 give relatively simple expressions for energy shifts E_{ij} as functions of the wire charges Q_j . In particular, tunneling of an electron onto the wire $j=1$ from the source contact will decrease the overall electrostatic energy of the system by

$$\mathbf{E}_{11} = \frac{e^2 C_0}{Z} \left(\frac{VC_{\text{dr}}}{e} - N - \frac{1}{2} \right) + \frac{e^2 C_2}{Z} \left(\frac{VC_{21}}{e} - N_1 - \frac{1}{2} \right), \quad (2)$$

with $Z = C_0(C_1 + C_2) + C_1 C_2$, total junction capacitance of a wire $C_j = C_{1j} + C_{2j}$, total charge on both wires $N = N_1 + N_2$, and total source and drain capacitances $C_{\text{sr}} = C_{11} + C_{12}$ and $C_{\text{dr}} = C_{21} + C_{22}$, respectively. Charging energies associated with all the other possible tunneling events can be found similarly.¹¹

Note that for $C_0 = 0$, Eq. (2) becomes a standard expression for the charging energy of a metal island in a double-junction system¹⁰ with single-wire junction capacitances. In this limit of negligible coupling, an electron tunneling on a particular wire does not feel the presence of the other wire, and all tunneling events for both wires sum up independently, as do the currents. In this case the Coulomb repulsion at low temperatures limits the maximum charge on each wire, which with increasing voltage increases stepwise by one elementary charge each time the voltage reaches critical values $V_{N_j} \cong e(N_j - \frac{1}{2})/C_{2j}$, where $N_j = 1, 2 \dots$ defines the maximum charge on the wire for voltages between V_{N_j} and $V_{N_{j+1}}$ at zero temperatures.

In the opposite limit of infinite coupling, e.g., $C_0 \rightarrow \infty$, both wires effectively constitute a single island, so the charging energy depends only on the total charge on both wires N . It is again described by the same standard double-junction expression, but with junction capacitances corresponding to the total source and drain junction capacitances C_{sr} and C_{dr} . Obviously, in this case the charging energy and the current do not depend on what particular wire an electron is actually tunnels, and the maximum allowed charge on both wires increases by one each time the voltage reaches

$$V_N \cong e(N^m - \frac{1}{2})/C_{\text{dr}}, \quad N^m = 1, 2 \dots \quad (3)$$

So that for $V_N < V < V_{N+1}$ at low enough temperatures, we always have $N \leq N^m$.

In the more interesting intermediate case, according to Eq. (2), each tunneling event “probes” (1) the whole array as a double-junction system with junction capacitances equal to the total drain/source capacitances and charged with the total charge N (the first terms in the square brackets), and (2) the particular wire on (from) which the tunneling is actually happening (the second terms in the brackets). The relative contribution of the terms is governed by the ratio of junction and coupling capacitances C_i/C_0 . In the case considered here, extremely small wire diameters yield junction capacitances on the order of 10^{-18} – 10^{-19} F, while the interwire capacitance for a typical wire length $\sim 1 \mu\text{m}$ is at least two orders of magnitude greater, i.e., $C_i/C_0 \leq 10^{-2}$.¹² In this case it is the total array charge N which matters for tunneling probabilities in the first place, and at low temperatures it is controlled by the Coulomb repulsion in the same way as the individual wire charges for uncoupled wires. One apparent consequence of this is a reduction of the critical voltages (and corresponding shrinking of the Coulomb-blockade region), since they are now determined by the total source capacitance $C_{\text{sr}} = \sum C_{1j}$. Attempts to apply this finding directly to our experimental system are, however, impeded by a present lack of knowledge of which specific wires in the array participate in the charge transport, and of a finite dispersion in oxide thickness and a large dispersion in junction resistances.

Thus from the viewpoint of external terminal response, the matter does not seem to be far from an ordinary complication of the simple SET phenomenon in a single uncoupled wire. When we look closer into the internal system response, things become more interesting. We show below that strong wire coupling under SET conditions may lead to the *spontaneous polarization* of neighboring wires, which can be described by the wire charge difference $P = N_1 - N_2$ (in units of the electron charge e). The characteristic energy of this “excitonic excitation” of the system, when an accumulation of excessive electrons on one wire is partly compensated for by the hole accumulation on another one, is controlled by the large interwire capacitance, and can be estimated as $E_P \sim (eP)^2/8C_0$. For $P \sim N$ it makes only a small contribution to the total charging energy of the system. Thus, for $V_n < V < V_{n+1}$, electrons entering the wires through the source junctions bring with them enough energy to excite a highly polarized state with $P \gg N^m$. This may in turn lead to externally observable effects such as rf radiation of the arrays when a constant bias voltage is applied.

We have examined this collective effect by (i) performing Monte Carlo simulations of the electron transport through the system using Eqs. (1) and (2) and similar expressions for the other tunneling energies, and (ii) using a master equation for analytical investigations at low temperatures. The latter is greatly simplified by an assumption of a strong asymmetry of the drain and source resistances, which is justified in the case of a considerable difference in thickness of the drain and source oxide junctions, and is also known to give a well-defined Coulomb staircase on the I - V characteristics of a single double-junction system. Typical values were used in modeling: junction capacitances $C_{ij} = (1.6 \pm 0.2) \times 10^{-19}$ F, coupling capacitance $C_0 = (0-200) \times C_{ij}$, junction resistances $R_{11} = R_{12} = R = 50$ k Ω (source), $R_{21} = 200R$, and $R_{22} = 200-2000) \times R$ (drain).

III. MONTE CARLO SIMULATIONS RESULTS

We investigated the Coulomb-controlled transport of electrons through the double-wire system shown in Fig. 1 by means of a simple Monte Carlo approach which is commonly employed to simulate SET effects.⁹ Starting with an initial wire charge configuration, our computer program uses Eq. (2) and similar equations to calculate separately energy shifts associated with tunneling of an electron in either direction through each of the four tunnel junctions, and then, using Eq. (1), calculates all eight tunneling rates (in two directions for each tunnel junction) for a given applied voltage. After that, the eight tunneling probabilities are calculated by normalizing each tunneling rate by the total rate of tunneling $\Gamma_{\text{tot}} = \sum \Gamma_{ij}$, with Γ_{tot}^{-1} defining the time step. An interval of unit length is then divided into eight contiguous sectors of the same proportions as the tunneling probabilities, and a random number from a unit interval is generated to determine which event actually takes place. A changed set of charging energies is calculated then in accordance with the changed charge configuration, and the procedure repeats. The resulting set of charging states represent the time evolution of the wire charges (and the transferred charge, which determines the electric current) with varying time step $1/\Gamma_{\text{tot}}$.

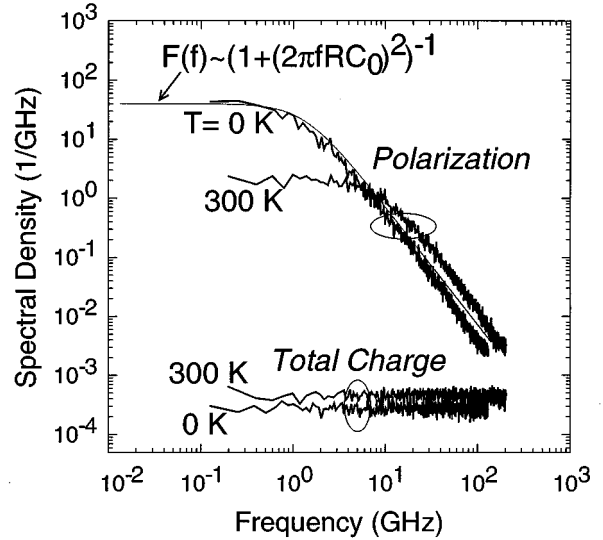


FIG. 2. Spectral density of fluctuations for the wire charge polarization P and the total wire charge N at $T=0$ and 300 K.

Figures 2–5 show the results of computer simulations of electron flow through the double-wire system as described by Eqs. (1) and (2). We found that, in the case of strong coupling, considerable interwire polarization does occur in certain voltage ranges. For identical wires this spontaneous polarization stochastically oscillates in time, with zero time average $\langle P \rangle$. Figure 2 shows the spectral density of these fluctuations for two different temperatures in comparison with the spectral density of the total charge noise $\langle |N(\omega)|^2 \rangle$. The big difference between the low-frequency intensities of the P and N noise comes partly from the difference in their bandwidths: while the polarization noise bandwidth is determined by a slow process of recharging of the large coupling capacitor with a characteristic time RC_0 ($R \sim R_{ij}$), noise of the total array charge N is spread out over much larger bandwidth determined by the junction capacitances. The difference appears even more striking at low temperatures, when a Coulomb blockade of tunneling par-

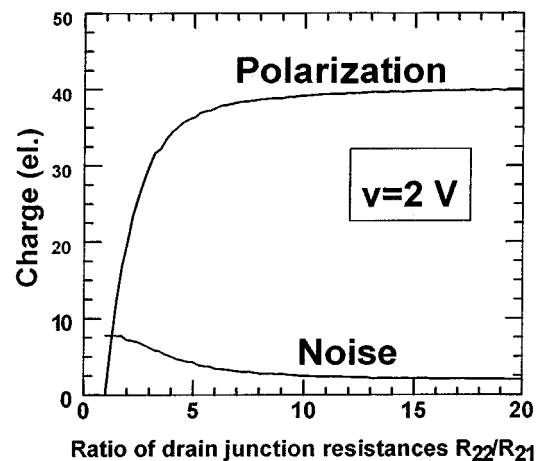


FIG. 3. Average interwire polarization of charge and polarization dispersion vs wire asymmetry.

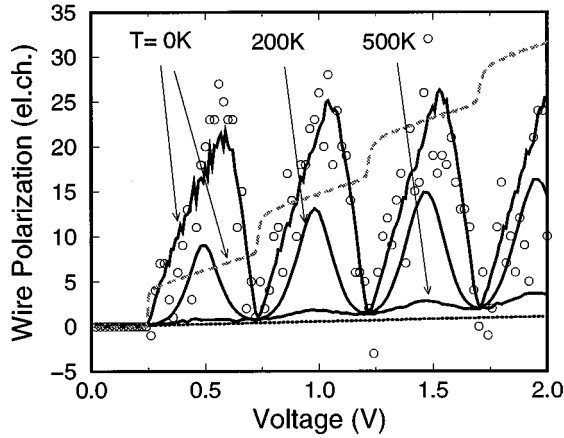


FIG. 4. Average interwire polarization $\langle P \rangle = \langle N_1 - N_2 \rangle$ vs voltage at three different temperatures. The dotted curve represents the interwire polarization in accordance with Kirchoff's laws. Circles represent the wire polarization at a particular time instant for $T=0$ K. For comparison, the I - V staircase at zero temperature is shown by a dashed line (arb. units).

tially suppresses the total charge noise while effectively increasing the polarization noise, as is shown in Fig. 2, where $\langle \Delta P^2 \rangle (\omega \approx 0)$ exceeds $\langle \Delta N^2 \rangle (\omega \sim 0)$ by more than three orders of magnitude.

The polarization becomes more regular in the case of *asymmetrical wires*, when either the source or drain junction resistances R_{ij} differs for different wires. If the second wire drain junction resistance is larger than that of the first wire, electrons will leave the first wire faster, thus yielding a positive charge (“holes”) accumulation on this wire and an electron accumulation on the “slower” wire. Figure 3 shows that $\langle P \rangle$ at first rapidly increases and then saturates with increasing wire asymmetry.

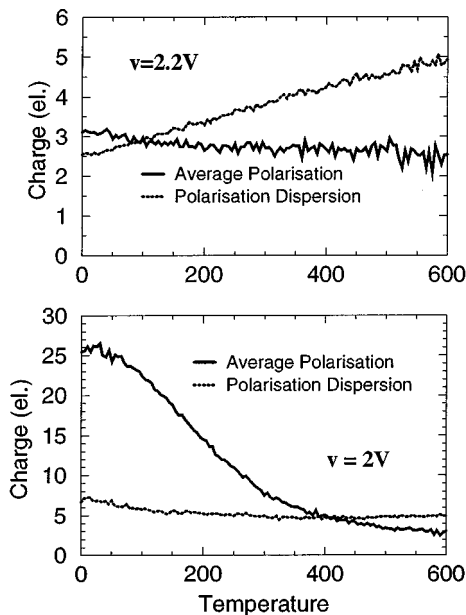


FIG. 5. Average charge polarization and the polarization dispersion vs temperature for different voltages: anomalous suppression of the polarization noise with temperature.

Both $\langle P \rangle$ and σ_P , however, are not constant for a given set of wire parameters, but periodically oscillate with increasing voltage (Fig. 4). It appears that they reach local minima at critical voltages described by Eq. (3), i.e., where infinitely strong coupled wires give steps on the N - V and I - V curves. The average wire charges at these voltages are determined approximately by Kirchoff's laws, and are almost independent of the system temperature.

The strong system polarization in between critical voltages, being the consequence of the Coulomb-controlled tunneling, does not exist for high temperatures relative to the charging energy, i.e., $kT \gg e^2/2C_j$, where the thermal fluctuations govern the charge statistics. For high temperatures the average wire charges approach Kirchoff's values for all voltages and vary almost linearly with the voltage (500 K—curves on Fig. 4).

For lower temperatures the polarization statistics is instead governed by the shot noise in combination with the Coulomb repulsion, which suppresses the fluctuations of the total charge on both wires but increases the anticorrelated fluctuations of the individual wire charges. This behavior is illustrated on Fig. 5 which shows how $\langle P \rangle$ and σ_P depend on temperature for two different voltages: one that corresponds to a local $\langle P \rangle$ minimum (the top graph), and another that gives a peak value of $\langle P \rangle$ for low temperature (the lower graph). In the first case the almost constant average polarization is accompanied by an increasing noise as temperature increases.

Surprisingly, in the second case, not only the average polarization, but also the polarization noise decrease at first as the temperature rises, and only at higher temperatures does the polarization noise start rising again due to the thermal contribution, eventually reaching the same level as in the first case.

This anomalous temperature dependence of the polarization fluctuations is even more evident for spectral characteristics as was shown above (Fig. 2). Since the spectral bandwidth of the SET-induced polarization noise is much smaller than that of the pure shot noise, and increases with temperature, the low-frequency polarization noise decreases much faster than the polarization dispersion as the temperature increases—in our case by a factor of 3 when the temperature increases from 0 to 300 K.

The results of numerical simulations can be explained next, and analytically, at least for $T=0$, by means of the master-equation approach, which relates the probability of finding a system in a given state (N_1, N_2) to the transition rates to and from this state. Before doing that, however, it is helpful to reexamine the equations for tunneling rates (1) and energy shifts (2), and draw some important conclusions directly from these.

IV. MAXIMUM POLARIZATION

First, in the case of high drain resistances, the system will spend most of the time in a state with maximum possible total charge $N=N_{\max}$, since a “refill” of the wire charge goes much faster than a draining if $N < N_{\max}$, where $N_{\max} = N^m$ for $P=0$ or $C_0 = \infty$.

Second, we note that there are two processes which set limits on the degree of polarization:

(1) Accumulation of holes on a wire can finally *open up* this wire for tunneling into it of an additional electron, thus making the total wire charge $N=N^m+1$ and obviously shutting off electron tunneling on the other wire. If holes accumulate on the first wire, the corresponding condition reads $E_{11}(N^m+1, N_1) \geq 0$, or

$$N_1 \leq (N_1^{\max})_1 \equiv \left[\frac{C_0}{C_2} \frac{V - V_{N+1}}{\Delta V} + C_{21} \frac{V}{e} + \frac{1}{2} \right] \\ \approx - \left[\frac{C_0}{C_2} \left(1 - \frac{V - V_N}{\Delta V} \right) - \frac{C_{21}}{C_{dr}} N_m \right] < 0, \quad (4)$$

where $\Delta V = V_{N+1} - V_N = e/C_{dr}$, and $[x]$ denotes maximum integer equal or less than x . Obviously, for N_2 we would have

$$N_2 \geq (N_2^{\max})_1 = N^m + 1 - (N_1^{\max})_1. \quad (5)$$

(2) Simultaneous accumulation of electrons on another wire can by itself finally block this wire for tunneling from the source contact, thus setting a maximum number of electrons on a wire; for the second wire, this condition is $E_{12}(N^m, N_1) \geq 0$, or

$$N_2 \leq (N_2^{\max})_2 \equiv \left[\frac{C_0}{C_1} \frac{V - V_N}{\Delta V} + C_{22} \frac{V}{e} + \frac{1}{2} \right], \quad (6)$$

with

$$N_1 \geq (N_1^{\max})_2 = N^m - (N_2^{\max})_2. \quad (7)$$

Note that, due to the large factor C_0/C_2 in the first term in the square brackets of Eq. (4), N_j^{\max} can greatly exceed the maximum total charge, which for zero polarization is given by

$$N^m = \left[\frac{VC_{dr}}{e} + \frac{1}{2} \right]. \quad (8)$$

Note also, that while the first mechanism leads to decreasing polarization with increasing voltage, the second one defines polarization limit which increases with voltage above V_N , and both predict polarization minimum at $V = V_N$.

Dotted lines in Fig. 6 show the polarization limits as defined by Eqs. (4–7). Comparing them with simulations result at $T=0$ for $\langle N_1 \rangle$ and $\langle N_2 \rangle$, which are given by solid lines, one can see that, while Eqs. (4) and (5) relatively well describe the descending part of the polarization curves, the increase of the average polarization goes slower than predicted by Eqs. (6) and (7). To describe the system behavior in this case, we will employ the master-equation approach.

V. MASTER-EQUATION APPROACH

In the general case, the polarization is driven by the shot noise of tunneling, and stochastically oscillates in time around some average value $\langle P \rangle$ which is defined by the degree of the wire asymmetry. While for strictly symmetrical wires ($C_{i1} = C_{i2}$ and $R_{i1} = R_{i2}$), obviously $\langle N_1 \rangle = \langle N_2 \rangle$, non-zero interwire polarization is required to compensate for wire asymmetry in steady-state conditions.

To find this stationary polarization, as well as the polar-

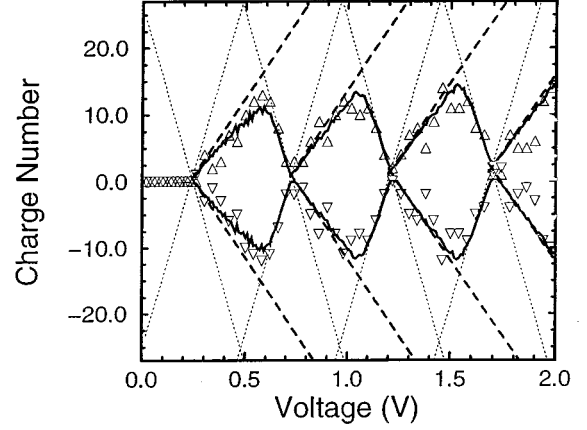


FIG. 6. Wire charges vs voltage as given by Monte Carlo simulations (solid line), polarization limits in accordance with Eqs. (4) and (5) (dotted lines), and average polarization given by the master-equation analysis [Eq. (25), dashed line].

ization noise for an arbitrary wire asymmetry, one has to obtain a probability function for the system to be in a certain charge state. In the case of strong interwire coupling, it is more appropriate to describe the state of the system in terms of total wire charge N and wire polarization P rather than individual wire charges N_1 and N_2 . While the latter are strongly coupled, random ‘‘motions’’ of N and P occur on completely different energy scales, and can therefore be decoupled from each other and described separately.

As above, we consider the case of a strongly asymmetric system with $R_{dr} \gg R_{sr}$ so that N almost always has time to reach its maximum value before an electron leaves the wires, and the system spends its time jumping between states with $N = N_{\max}$ and $N_{\max} - 1$. However, the polarization P varies over a much wider range, and its behavior is reminiscent of the diffusion of a particle in a potential well when it is driven by a random force—the shot noise of tunneling in this case. If the maximum wire charge $N_{\max} = N^m$, i.e., conditions (4) are not yet fulfilled, the corresponding steady-state distribution can be found, in some approximations, in a closed form.

The probability $\rho(N, P)$ for the system to be in a state (N, P) with $N = N_{\max}$ can change either by tunneling of an electron *on* either of the wires from states $(N_1 - 1, N_2) \equiv (N - 1, P - 1)$ or $(N_1, N_2 - 1) \equiv (N - 1, P + 1)$, or by tunneling of an electron *from* either of the wires:

$$\dot{\rho}(N_{\max}, P) = \rho(N_{\max} - 1, P - 1) \mathfrak{J}_{1-}(N_{\max} - 1, P - 1) \\ + \rho(N_{\max} - 1, P + 1) \mathfrak{J}_{2-}(N_{\max} - 1, P + 1) \\ - \rho(N_{\max}, P) [\mathfrak{J}_{1+}(N_{\max}, P) + \mathfrak{J}_{2+}(N_{\max}, P)]. \quad (9)$$

where $\mathfrak{J}_{i-}(N, P)$ denotes the rate of tunneling of an electron *onto* the i th wire, and $\mathfrak{J}_{i+}(N, P)$ is the electron tunneling rate *from* the i th wire if the system is currently in the state (N, P) . In the case of zero temperature, which we will consider for simplicity below,

$$\mathfrak{J}_{i+}(N,P) = \Gamma_{2i}(N_1, N_2), \quad \mathfrak{J}_{i-}(N,P) = \Gamma_{1i}(N_1, N_2), \quad (10)$$

where $N = N_1 + N_2$ and $P = N_1 - N_2$. Similarly, for $\rho(N_{\max} - 1, P')$, one can write

$$\begin{aligned} \dot{\rho}(N_{\max} - 1, P') &= \rho(N_{\max}, P' + 1) \mathfrak{J}_{1+}(N_{\max}, P' + 1) \\ &+ \rho(N_{\max}, P' - 1) \mathfrak{J}_{2+}(N_{\max}, P' - 1) \\ &- \rho(N_{\max} - 1, P') [\mathfrak{J}_{1-}(N_{\max} - 1, P') \\ &+ \mathfrak{J}_{2-}(N_{\max} - 1, P')], \end{aligned} \quad (11)$$

Substituting $P + 1$ and $P - 1$ into this equation instead of P' , we obtain a pair of equations which, together with Eq. (7), constitutes a complete set. In steady-state conditions, when all time derivatives are set to zero, using Eq. (11) one can easily express $\rho(N_{\max} - 1, P')$ through the probability function at $N = N_{\max}$,

$$\begin{aligned} \rho(N - 1, P') &= \rho(N, P' + 1) \frac{\mathfrak{J}_{1+}(N, P' + 1)}{\mathfrak{J}_{\Sigma-}(N - 1, P')} \\ &+ \rho(N, P' - 1) \frac{\mathfrak{J}_{2+}(N, P' - 1)}{\mathfrak{J}_{\Sigma-}(N - 1, P')}. \end{aligned} \quad (12)$$

Substituting this for $P' = P \pm 1$ in Eq. (9), we finally find an equation for the polarization probability $\rho(P) = \rho(N_{\max}, P)$:

$$A\rho(P) + B\rho(P - 2) + C\rho(P + 2) = 0, \quad (13)$$

where

$$\begin{aligned} A &= \frac{\mathfrak{J}_{1+}(N, P) \mathfrak{J}_{1-}(N - 1, P - 1)}{\mathfrak{J}_{\Sigma-}(N - 1, P - 1)} \\ &+ \frac{\mathfrak{J}_{2+}(N, P) \mathfrak{J}_{2-}(N - 1, P + 1)}{\mathfrak{J}_{\Sigma-}(N - 1, P + 1)} - \mathfrak{J}_{\Sigma+}(n, P), \end{aligned} \quad (14)$$

$$B = \frac{\mathfrak{J}_{2+}(N, P - 2) \mathfrak{J}_{1-}(N - 1, P - 1)}{\mathfrak{J}_{\Sigma-}(N - 1, P - 1)}, \quad (15)$$

$$C = \frac{\mathfrak{J}_{1+}(N, P + 2) \mathfrak{J}_{2-}(N - 1, P + 1)}{\mathfrak{J}_{\Sigma-}(N - 1, P + 1)}, \quad (16)$$

and

$$\mathfrak{J}_{\Sigma\pm}(N, P) = \mathfrak{J}_{1\pm}(N, P) + \mathfrak{J}_{2\pm}(N, P).$$

Due to the very weak dependence of charging energies and tunneling rates on the polarization P , one can reasonably expect probability ρ to be a slow function of polarization, so that the finite difference equation (13) can be replaced by a differential equation using the expansion

$$\rho(P \pm 2) = \rho(P) \pm 2\rho'_P(P) + 2\rho''_{PP}(P), \quad (17)$$

that gives

$$a\rho(P) + 2b^- \rho'_P(P) + 2b^+ \rho''_{PP}(P) = 0, \quad (18)$$

with

$$\begin{aligned} a &= A + B + C, \\ b^- &= C - B, \\ b^+ &= C + B. \end{aligned} \quad (19)$$

To solve this equation, one has to find the coefficients a, b^- , and b^+ explicitly from Eqs. (14)–(19). Assuming for simplicity that all the junction capacitances are equal,

$$C_{11} = C_{12} = C_{21} = C_{22} = C \ll C_0,$$

and using Eq. (10), one can write the tunneling rates in the form

$$\begin{aligned} \mathfrak{J}_{1-}(N, P) &= \frac{1}{R_{11}} \theta[\gamma_-(N) - \gamma_0 P], \\ \mathfrak{J}_{1+}(N, P) &= \frac{1}{R_{21}} \theta[\gamma_+(N) + \gamma_0 P], \end{aligned} \quad (20)$$

$$\mathfrak{J}_{2-}(N, P) = \frac{1}{R_{12}} \theta[\gamma_-(N) + \gamma_0 P],$$

$$\mathfrak{J}_{2+}(N, P) = \frac{1}{R_{22}} \theta[\gamma_+(N) - \gamma_0 P],$$

where $\theta[x] = x$ for $x > 0$, and 0 otherwise:

$$\begin{aligned} \gamma_{\pm}(N) &= \frac{1}{4C} \left[\frac{2VC}{e} - \frac{1}{2} \left(1 + \frac{C}{C + C_0} \right) \pm N \right] \\ &\cong \frac{1}{4C} \left(\frac{2VC}{e} - \frac{1}{2} \pm N \right), \end{aligned} \quad (21)$$

$$\gamma_0 = \frac{1}{4(C + C_0)} \cong \frac{1}{4C_0}. \quad (22)$$

Note that $e^2 \gamma_{\pm}(N)$ is equal to the energy change associated with tunneling of an electron onto/from the wires with total charge N on them, if they were galvanically connected to each other (i.e., the coupling capacitance $C_0 = \infty$).

Assuming further that the source junction resistances are equal, i.e., $R_{11} = R_{12}$, from Eqs. (18)–(22) one can finally find an equation for the polarization probability in an explicit form,

$$\rho(P) + (P - \alpha x) \rho'_P(P) + (x - \alpha P) \rho''_{PP}(P) = 0, \quad (23)$$

where

$$\alpha = \frac{R_{21} - R_{22}}{R_{22} + R_{21}} \quad (24)$$

reflects the asymmetry between wires, and

$$x = \frac{\gamma_+(N) \gamma_-(N - 1) + \gamma_0^2 P^2}{(\gamma_+(N) + \gamma_-(N - 1)) \gamma_0}. \quad (25)$$

We can further simplify this equation by considering only slightly asymmetrical drain resistances and neglecting αP with respect to x in the last term of Eq. (23), and $\gamma_0^2 P^2$ in the nominator of Eq. (25). Equation (23) can be then readily solved, yielding a Gaussian function for the polarization probability,

$$\rho(P) \propto \exp\left(-\frac{(P - \langle P \rangle)^2}{2\sigma_P^2}\right), \quad (26)$$

with the average polarization $\langle P \rangle = \alpha x$, and the polarization dispersion $\sigma_P^2 = x(1 - \alpha^2)$. Expression (25) for x can be

simplified by rewriting it in terms of characteristic voltage $V_N = (e/2C)(N^m - \frac{1}{2})$. Then $\gamma_+(N_{\max})$ and $\gamma_-(N_{\max}-1)$ become simply

$$\gamma_+(N) = \frac{V + V_N}{2e},$$

$$\gamma_-(N) = \frac{V - V_N}{2e}.$$

Substituting these expressions into Eq. (25), we find

$$x = \frac{C_0}{eV} (V^2 - V_N^2), \quad (27)$$

and, finally, for the average polarization,

$$\langle P \rangle = \alpha \frac{C_0}{eV} (V^2 - V_N^2), \quad (28)$$

and for the polarization dispersion,

$$\sigma_P = \left(\frac{C_0}{eV} (V^2 - V_N^2) (1 - \alpha^2) \right)^{1/2}. \quad (29)$$

From Eqs. (28) and (29) we easily find $\langle N_j \rangle = (\langle N \rangle \pm \langle P \rangle)/2$, and $\sigma_{N_j} = \sigma_P/2$. In Fig. 6 these average wire charges as defined from Eq. (28) are shown by the dashed lines for $N=1, 2, 3$, and 4, and, as one can see, they well describe the initial increase in average polarization as the voltage increases above V_N . A polarization increase with voltage, however, will finally lead to an opening of the positively charged wire for tunneling of an additional electron and increase of the maximum possible N from N^m to $N^m + 1$, which happens at voltages corresponding in Fig. 6 to intersections of the dotted and dashed curves. This set of characteristic voltages, which we will denote as V_N^* , can be easily estimated from Eqs. (4) and (28),

$$V_N^* \approx V_N + \frac{\Delta V}{1 + \alpha}. \quad (30)$$

As mentioned in Sec. IV, this will close off the negatively charged wire for tunneling, and the polarization will slowly decay until the negatively charged wire opens for tunneling again. That in turn will increase the polarization, and the system will thus oscillate around the average polarization given by Eqs. (4) and (5), as is clearly seen in Fig. 6 for voltages slightly lower than V_N .

The correspondence of analytical results and computer simulations is also relatively good for the polarization dispersion. Figure 7 shows by a dotted line the wire polarization dispersion as given by Eq. (29), together with the results of Monte Carlo simulations for symmetrical wires (solid line), and asymmetrical wire drain resistances as in Fig. 5 (dashed line). For comparison, the long-dashed curve in Fig. 6 gives the charge dispersion at high temperatures. As one can see, the effect of SET is to increase the polarization (and fluctuations) of wire charges in some voltage regions, and to suppress them in others.

An important question is the observability of the polarization effect from ‘‘outside’’ the nanoarray, e.g., by measuring the current. The average current is given in the general case as

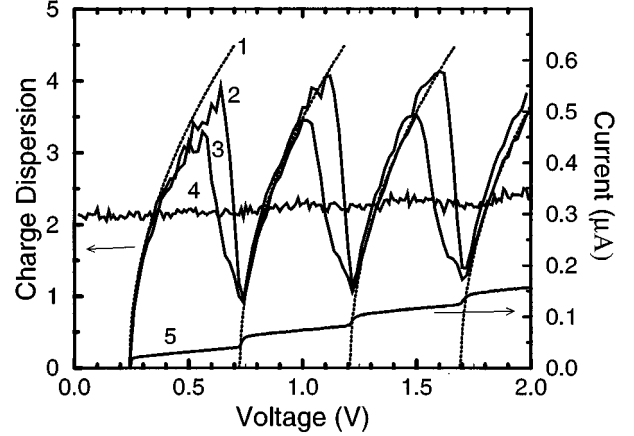


FIG. 7. Results of master-equation (ME) analysis and Monte Carlo calculations (MC) for the polarization dispersion. Curves 1 and 3 show the predictions of the ME approach and the results of the MC simulations for $R_{12}/R_{22}=0.4$ and $T=0$ K. Curve 2 shows the simulation results for equal drain resistances at $T=0$ K. Curve 4 represents the polarization noise at high temperature. For comparison, the I - V staircase is shown in the figure by curve 5.

$$\langle I \rangle = e \int dP dN \rho(N, P) (\mathfrak{I}_{1+}(N, P) + \mathfrak{I}_{2+}(N, P)). \quad (31)$$

In the case when system spends most of its time in the state with $N=N_m$, i.e., in regions where polarization increases with voltage, we have, using Eqs. (20), (24), and (28),

$$\begin{aligned} \langle I \rangle &= \frac{1}{R_{\text{dr}}} \left(\frac{V + V_N}{2} + \alpha e \gamma_0 \langle P \rangle \right) \\ &= \frac{V(1 - \alpha^2) + V_N \left(1 + \alpha^2 \frac{V_N}{V} \right)}{2R_{\text{dr}}}. \end{aligned} \quad (32)$$

According to this expression, the polarization effectively decreases the system differential conductance dI/dV in the corresponding voltage regions, which is reduced to zero or even slightly negative values for $\alpha \rightarrow 1$, i.e., when one of the wires is effectively isolated from the drain electrode. This wire acts then as an effective ‘‘stopper’’ of the tunneling current through the other one as well.

However, the change in differential conductance is on the order of α^2 and requires a very strong asymmetry between wires to be visible. Indeed, this is clearly seen in Fig. 8(a), which shows the system I - V characteristics for $R_{21}=R_{22}$ (upper curve), $R_{21}=0.6R_{22}$ (middle), and $R_{21}=0.1R_{22}$ (lower) and equal R_{dr} . It also shows a *reduction* in the system differential resistance in regions where polarization decreases with voltage, which can be explained by noting that in these regions there is a nonzero probability for the system to be in the state with an additional electron, i.e., with $N=N_m+1$, and this probability increases with increasing voltage, as illustrated by the rising fluctuations of the total wire charge N in Fig. 8(b). The rising probability to transfer an additional electron through the system should give a *de-*

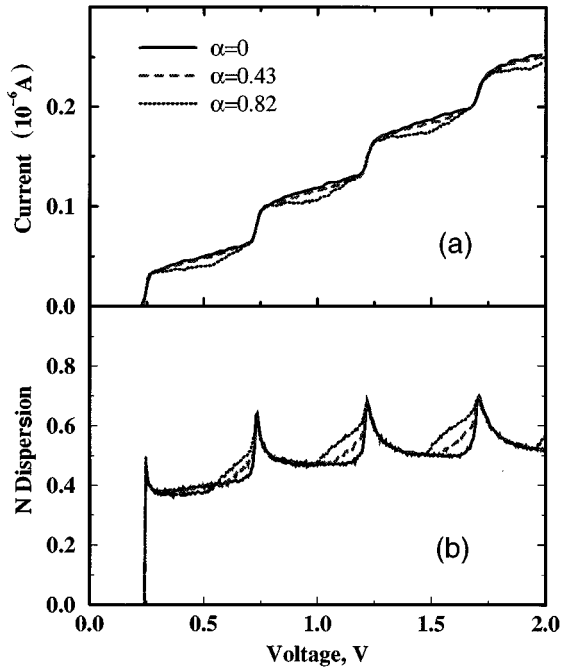


FIG. 8. Current-voltage characteristics of the double-wire system (a), and fluctuation dispersion of the total charge on both wires (b) depending on interwire asymmetry.

creased differential resistance, with the effect being the more pronounced the higher the wire asymmetry. Indeed, using Eqs. (4) and (5) and assuming equal capacitances of the tunnel junctions, for the polarization we find a simple expression

$$P \approx 2C_0 \frac{V_{N+1} - V}{e},$$

which gives

$$\langle I \rangle = \frac{V(1 + \alpha) + V_N - \alpha V_{N+1}}{2R_{dr}},$$

with the increased differential conductance. We thus find that the system I - V characteristics become more complicated when the wires become polarized, and an additional critical

voltage point V_N^* appears in between Coulomb steps V_N and V_{N+1} . This adds an interesting “twist” to the otherwise expected changes in external I - V dependence, such as a down-scaling of the critical voltages of Coulomb steps in the presence of strong coupling.

VI. CONCLUSIONS

We investigated the effect of wire coupling on Coulomb-controlled tunneling for a two-wire double-junction system, and developed a theory of spontaneous interwire polarization which occurs in the case of strong interwire coupling. The theory can be used as a basis for treatment of SET effects in strongly coupled nanowires such as in the arrays being fabricated electrochemically in our labs. The predicted spontaneous charge polarization could lead to interesting and externally observable effects such as a nonmonotonic differential resistance measurable in external terminal I - V characteristics, and a possible electromagnetic radiation from the charge-polarization “waves” when a constant external bias is applied to an array of nanowires.

An important question remains unanswered, of whether these “polarization waves,” which should exist in nanowire arrays under SET conditions, are purely stochastic or some sort of polarization order can result from the Coulomb interactions between the wire charges and possibly external electric field, and deserves additional considerations which are currently underway. These considerations should also include an important effect which is untouched upon in the present model, namely, the so-called cotunneling, or macroscopic quantum tunneling of charge.¹³ This effect, which for a single double-junction system yields a nonvanishing current below the Coulomb-blockade voltage, in the case of two or more coupled systems may lead to more complex consequences due to the possible spontaneous accumulation of charge on the wires in the Coulomb-blockade region.

ACKNOWLEDGMENTS

A.T. and J.X. are grateful to K. K. Likharev, S. Luri, and A. N. Korotkov for helpful and interesting discussions. This work was supported by grants from National Science and Engineering Research Council and Ontario Laser and Lightwave Research Center.

*E-mail: tager@vrg.toronto.edu

¹D. Al-Mawlawi, C. Z. Liu, and M. Moskovits, *J. Mater. Res.* **9**, 1014 (1994).

²D. Al-Mawlawi, C. Douketis, T. Bigioni, M. Moskovits, D. Routkevich, L. Ryan, T. Haslett, A. Williams, and J. M. Xu, in *Proceedings of the Symposium on Nanostructured Materials and Electrochemistry, 187th Meeting of the Electrochemical Society, Reno, NV, 1995* (The Electrochemical Society, Pennington, NJ, 1995), Vol. 95, p. 262.

³D. Routkevich, T. Bigioni, M. Moskovits, and J. M. Xu, *J. Phys. Chem.* **100**, 14 037 (1996).

⁴D. Al-Mawlawi, M. Moskovits, D. Ellis, A. Williams, and J. M. Xu, in *Proceedings of the International Semiconductor Research Symposium, Charlottesville, 1993* (University of Virginia, Charlottesville, 1993), p. 311.

⁵J. E. Mooij and G. Schön, in *Single Charge Tunneling, Coulomb*

Blockade Phenomena in Nanonstructures, Vol. 294 of *NATO Advanced Study Institute, Series B: Physics*, edited by H. Grabert and M. H. Devoret (Plenum, New York, 1992), p. 275.

⁶A. A. Tager, M. Lu, M. Moskovits, and J. M. Xu, *Phys. Low-Dim. Struct.* **12**, 149 (1995).

⁷A. A. Tager, M. Lu, J. M. Xu, and M. Moskovits, in *Extended Abstracts of the International Conference on Solid State Devices and Materials, Osaka, 1995* (Japan Society for Applied Physics, Tokyo, 1995).

⁸D. V. Averin, A. N. Korotkov, and Yu. V. Nazarov, *Phys. Rev. Lett.* **66**, 2818 (1991).

⁹K. Mullen, E. Ben-Jacob, R. C. Jaklevic, and Z. Schuss, *Phys. Rev. B* **37**, 98 (1988).

¹⁰D. V. Averin and K. K. Likharev, in *Mesoscopic Phenomena in Solids*, edited by B. Altshuler, P. A. Lee, and R. A. Webb (Elsevier, Amsterdam 1991), Chap. 6.

¹¹Tunneling through the junction [Eq. (21)] from the first wire onto the right contact layer yields system energy shift \mathbf{E}_{21} , which can be found from the \mathbf{E}_{11} by changing all Q 's to $-Q$, $C_{dr} \rightarrow C_{sr}$ and $C_{21} \rightarrow C_{11}$. Similarly, tunneling onto the second wire is associated with the energy shift \mathbf{E}_{12} that can be found from the \mathbf{E}_{11} simply by changing $C_2 \rightarrow C_1$ and $C_{21} \rightarrow C_{22}$. For \mathbf{E}_{22} then, all we have to do is to change signs of the Q 's and make replacements $C_{dr} \rightarrow C_{sr}$ and $C_{22} \rightarrow C_{11}$. Energy shifts \mathbf{E}_{ij} due to tunneling in the opposite direction are then $\mathbf{E}_{ij}(Q, Q_j, V) = \mathbf{E}_{ij}(-Q, -Q_j, -V)$.

¹²This estimation should be seen as a lower limit of the wire-contact electrode capacitance. In the case of a single free-standing wire, the self-capacitance of the wire has to be added to

the junction capacitance when considering charging energies. This capacitance increases with wire length as $L/\ln(L)$, and therefore the interwire capacitance–junction capacitance ratio C_i/C_0 would be at least an order of magnitude higher than assumed. However, when placed in a nanowire array, a wire is shielded by its neighbors, and the wire-ground capacitance should be to a large extent reduced. The problem of a large wire-ground capacitance in this case is shifted to the array's boundary conditions, whose effect on the ‘‘inner’’ wires requires a separate examination and is beyond the scope of the paper.

¹³D. V. Averin and Yu. V. Nazarov, in *Single Charge Tunneling, Coulomb Blockade Phenomena in Nanonstructures* (Ref. 5), pp. 217–247.